

Solar wind density control of energy transfer to the magnetosphere

R. E. Lopez,¹ M. Wiltberger,² S. Hernandez,¹ and J. G. Lyon³

Received 6 October 2003; revised 9 March 2004; accepted 17 March 2004; published 17 April 2004.

[1] It is generally believed that the coupling of energy between the solar wind and the magnetosphere depends almost exclusively on the solar wind speed and magnetic field, with density and temperature playing little or no role. However, recent studies have indicated that under certain conditions, such as the main phase of a storm, density can have a significant role in modulating the transfer of energy to the magnetosphere. In this paper we demonstrate the effect using global MHD simulations of the solar wind-magnetosphere interaction. We also identify the physical mechanism that leads to the density control, namely the modification of the compression ratio of the bow shock, and explain why it is only apparent during periods of strong, southward IMF. *INDEX TERMS:* 2431 Ionosphere: Ionosphere/magnetosphere interactions (2736); 2753 Magnetospheric Physics: Numerical modeling; 2784 Magnetospheric Physics: Solar wind/magnetosphere interactions. *Citation:* Lopez, R. E., M. Wiltberger, S. Hernandez, and J. G. Lyon (2004), Solar wind density control of energy transfer to the magnetosphere, *Geophys. Res. Lett.*, 31, L08804, doi:10.1029/2003GL018780.

1. Introduction

[2] The source of the energy that drives magnetospheric processes is the solar wind, and quantifying the transfer of energy from the solar wind to the magnetosphere is a fundamental problem in space physics. Reconnection plays a major role in the energy transfer process, and the simplest coupling function, the solar wind speed times the southward component of the IMF (VB_S), has proved to be an effective measure of energy transfer [Gonzalez, 1990]. Another widely used measure of the coupling is the epsilon parameter [Akasofu, 1981], which represents essentially the rectified Poynting flux in the solar wind. While these functions are not rigorously derived, Koskinen and Tanskanen [2002] point out that that epsilon is a useful first order approximation to the energy transfer, especially during substorms.

[3] While some of the coupling functions discussed by Gonzalez [1990] involve the solar wind density, only those involving V and B are widely used. Siscoe *et al.* [2002] have pointed to an important role for the solar wind pressure in relationship to the saturation of the polar cap potential, however, that is not the issue that we are addressing here. In fact, numerous empirical studies continue to provide the same result that what seems to matter the most for the overall

coupling is something like epsilon or VB_S . For example, Boyle *et al.* [1997] constructed an empirical function to describe the polar cap potential solely as a function of solar wind speed, magnetic field, and the angle between the field and the Z direction. In fact, Boyle *et al.* [1997] point out the potential has an “insignificant” dependence on solar wind pressure. Similarly, although Weimer [2001] did include solar wind pressure in an empirical model of the polar cap potential, a function involving only V and B provided an excellent ($r = 0.98$) correlation with the potential.

[4] Given this body of literature, one might find it surprising that variations in solar wind density could have a significant impact on solar wind-magnetosphere coupling. However, Shue and Kamide [2001] showed that from 0600 UT to 1200 UT on January 10, 1997, the solar wind density controlled the variations in the westward electrojet. A similar behavior was noted in an MHD simulation of the event [Goodrich *et al.*, 1998]. Moreover, Palmroth *et al.* [2004] found a solar wind density dependence in the overall magnetospheric dissipation calculated in their MHD simulations. In the next section we will explore this result and provide a simple physical explanation as to why density can affect the energy coupling from the solar wind to the magnetosphere.

2. MHD Simulations of Density-Controlled Dissipation

[5] This study uses the Lyon-Fedder-Mobarry (LFM) global MHD code, which models the global solar wind-magnetosphere interaction [e.g., Goodrich *et al.*, 1998]. Previous studies using solar wind data to drive the simulation have demonstrated that the code produces realistic storm and substorm behavior [Lopez *et al.*, 2001; Wiltberger *et al.*, 2000]. The January 10, 1997 was one of the storms simulated and compared to observations, and as mentioned above, Goodrich *et al.* [1998] noted that during the main phase of the storm, higher values of solar wind density were correlated with larger overall values of field aligned currents and simulated auroral emissions.

[6] Figure 1 shows the correlation coefficient (from 0600 UT to 1200 UT, following Shue and Kamide [2001]), between the integrated Joule heating in the northern ionosphere (see Slinker *et al.* [1999] for details on the LFM ionospheric simulation) and the solar wind density. We can see that there is a very good correlation from 0600 UT to 1200 UT (which corresponds to the period when the solar wind magnetic field was strongly southward), in accord with the Shue and Kamide [2001] result.

[7] To explore this further, we ran a set of simulations that initially have $V = 400$ km/s, $n = 2$ cm⁻³ or 5 cm⁻³, $B_Z = -5$ nT ($B_X = B_Y = 0$), and C_s (sound speed) = 40 km/s. At 0200 (simulation time) B_Z was decreased to -20 nT. At 0300 a 15-min density pulse ($n = 15$ cm⁻³) was introduced

¹Department of Physics, University of Texas, El Paso, Texas, USA.

²High Altitude Observatory, National Center for Atmospheric Research, Boulder, Colorado, USA.

³Department of Physics and Astronomy, Dartmouth College, Hanover, New Hampshire, USA.

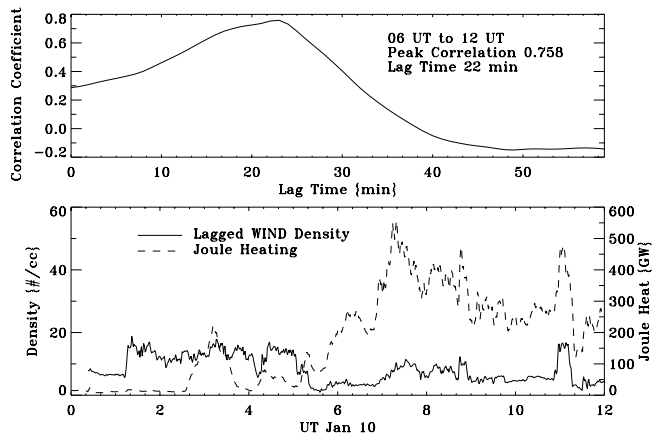


Figure 1. The bottom panel shows the integrated Joule heating in the northern ionosphere in the simulation along with the solar wind density. The top panel shows the correlation between the solar wind density and the Joule heating for the period 0600 UT to 1200 UT as a function of lag time, where zero lag is the time of solar wind entry onto the grid upstream of the bow shock.

into the two the runs. Figure 2 shows the integrated ionospheric Joule heating for these two runs. We can see that prior to 0200, when B_Z was -5 nT, the level of dissipation was the same for both the 2 cm^{-3} and 5 cm^{-3} runs. However, when B_Z becomes strongly negative at 0200, the dissipation levels separate with the higher density run experiencing a higher level of ionospheric Joule heating. When the density pulse hits, the dissipation peaks at roughly the same level, with the differences probably due to second-order effects such as differing conductivities. Thus it is clear that, during strongly southward IMF, higher solar wind densities produce higher levels of dissipation.

[8] The increased dissipation is driven by an increased polar cap potential, which is driven by the dayside reconnection rate. We can directly sample the simulation reconnection rate by plotting in Figure 3 the potential along the boundary between open and closed field lines (the rate at which flux crosses that boundary) for two time steps during

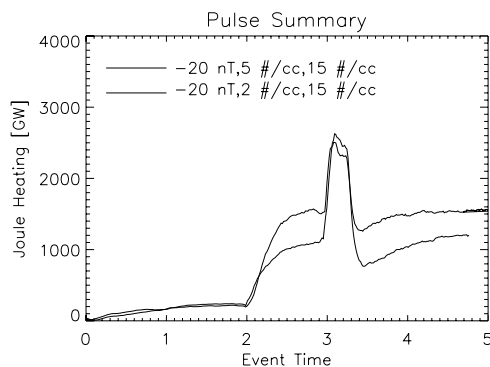


Figure 2. Integrated ionospheric Joule heating in the simulation for two runs as described in the text. The thin line has $n = 2 \text{ cm}^{-3}$ while the bold line has $n = 5 \text{ cm}^{-3}$. Both runs begin with $B_Z = -5$ nT; both decrease B_Z to 20 nT at 0200 UT and introduce a 15 cm^{-3} pressure pulse at 0300 UT.

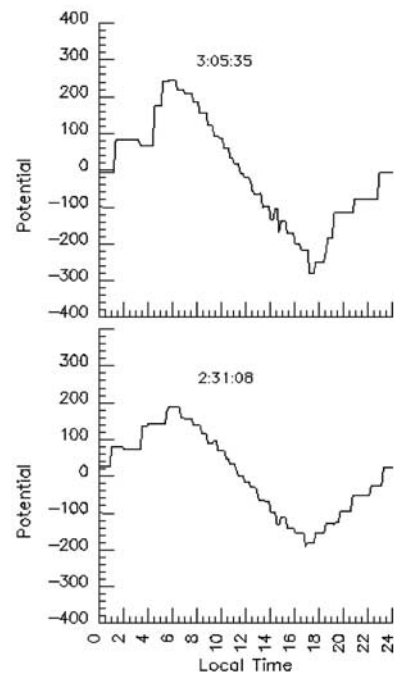


Figure 3. Ionospheric potential along the boundary between open and closed field lines in $n = 5 \text{ cm}^{-3}$ run with the pulse beginning at 0300.

the 5 cm^{-3} run. We can see that the reconnection rate increases at the time of the pressure pulse. We also note that the values of the polar cap potential are much higher than actually observed (about 550 kV at 0305). The LFM typically produces potential values that are a factor of 2 larger than those predicted by empirical models [Slinker *et al.*, 1999].

[9] Figure 4 presents B_Z in the simulation for the same two time steps in Figure 3, with the color bar set so that the negative solar wind and magnetosheath values can be discriminated. We can see that at 0305, during the time of the density pulse, the magnetosheath magnetic field was more strongly southward than earlier, yet the upstream solar wind magnetic field had not changed. This enhanced southward magnetosheath field was associated with the greater reconnection rate seen in Figure 3.

3. The Role of the Bow Shock

[10] As the solar wind crosses the bow shock, it is compressed and heated, with the amount of compression depending on the upstream fast mode speed. Generally, in space physics it is assumed that the Earth's bow shock is a high Mach number shock and that the compression ratio is a factor of 4 [e.g., Kallio and Koskinen, 2000]. For nominal values in the solar wind ($B = 5$ nT, $n = 5 \text{ cm}^{-3}$) the Alfvén speed is about 48.8 km/s. However, for the same density, if B is 20 nT, the Alfvén speed is about 200 km/s, and for moderate solar wind speed ($V = 400$ km/s) this produces a low Mach number shock. Inspecting Figure 4, we can see that when the density was 15 cm^{-3} the compression ratio was essentially a factor of 4, but during the earlier period with $n = 5 \text{ cm}^{-3}$, the compression ratio was about 2.5. A higher compression ratio means that a larger fraction of solar wind kinetic energy is converted into magnetic energy

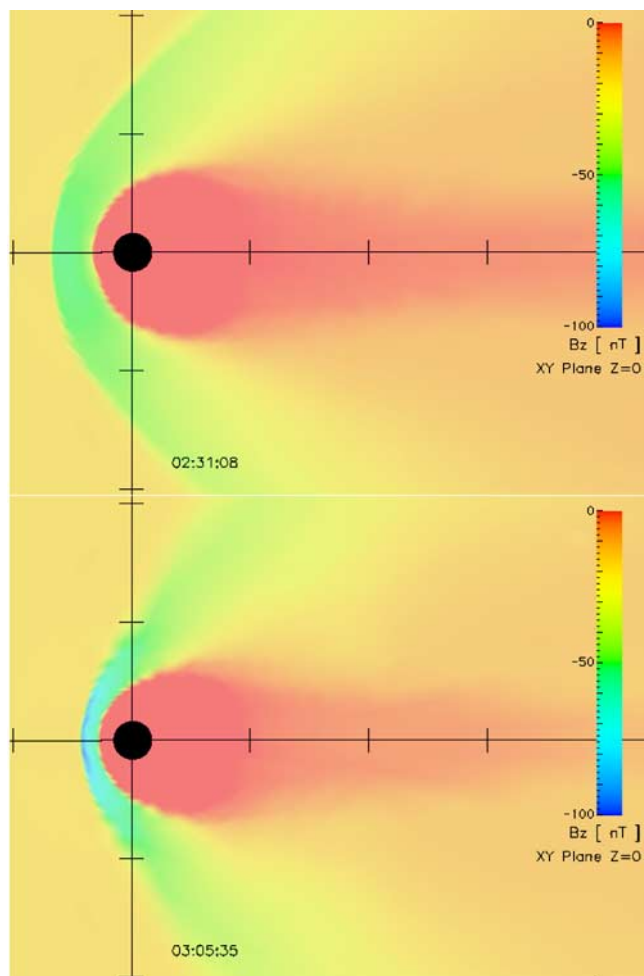


Figure 4. B_z in the equatorial plane for the simulation. The tic marks are at 20 RE intervals.

as the solar wind crosses the shock, so that a greater amount of magnetic energy is available in the magnetosheath.

[11] The physics of perpendicular MHD shocks is a well-known textbook problem [Boyd and Sanderson, 1969]. The compression ratio, r , may be calculated as function of the upstream parameters. But if the density increases, the Alfvén speed drops and the Mach number increases, as does the compression ratio. Figure 5 shows the compression ratio across a plane, perpendicular MHD shock as a function of the upstream density for a number of values of the upstream magnetic field, using $V = 400$ km/s, $C_s = 40$ km/s, and taking $\gamma = 5/3$. For values of the upstream magnetic field corresponding to typical IMF values, r is fairly insensitive to changes in the density. However, for high values of the upstream magnetic field, r becomes significantly dependent on the upstream density.

4. Interpretation and Conclusions

[12] During periods of strongly southward IMF, the compression ratio of the low Mach number shock is strongly affected by the variation in number density, so that even when the solar wind magnetic field is steady, higher densities result in a larger compression ratio across the shock, which produces larger magnetosheath fields. Thus a

stronger magnetic field is applied to the magnetopause, increasing the rate of transfer of magnetic flux across the open-closed field line boundary, resulting in a larger polar cap potential and more dissipation. The details of how various factors affecting the reconnection rate change, or the relationship of this effect to the saturation of the polar cap potential [Siscoe *et al.*, 2002] are beyond the scope of this paper. Nonetheless, significant changes in the magnetospheric energy dissipation rate can occur under conditions of steady IMF, all driven by the density-dependent mechanism described here.

[13] So why has this effect not been noticed, with all of the empirical studies pointing to VB_S or similar expressions controlling the coupling and little apparent density dependence? Most of the solar wind is in the high Mach number regime, so if one investigates the magnetospheric response to the solar wind, almost all of the data available will be during periods when the bow shock compression ratio is fairly insensitive to changes in solar wind density. However, if one wishes to accurately describe the coupling during magnetic storms, when the IMF is large and southward, the density effect could be very important, as during 0600 UT to 1200 UT on January 10, 1997, when the shock compression ratio (for a plane MHD shock) ranged from 2.49 to 3.54.

[14] On the other hand, during large, but northward, IMF, such as at the end of the magnetic cloud on January 11, 1997, when the densities were among the highest ever

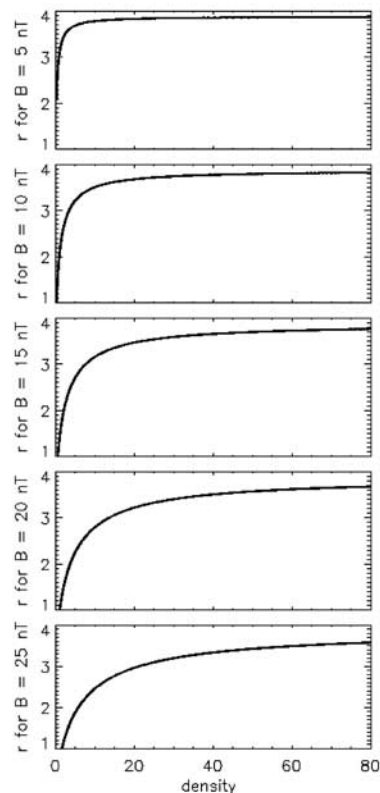


Figure 5. The compression ratio across the shock as a function of upstream density for various values of B_z in the upstream magnetic field as calculated for the case of a plane, perpendicular MHD shock.

measured, there was not a concomitant magnetospheric response. This is because the effect is not an issue strictly of the solar wind kinetic energy flux. Rather, it is a question of the amplification of the solar wind magnetic field by the bow shock, which is in essence a conversion kinetic energy to magnetic energy. However, the magnetic energy impacting the magnetopause is not very geoeffective if the field is northward.

[15] **Acknowledgments.** This material is based upon work supported by CISM, which is funded by the STC Program of the National Science Foundation under Agreement Number ATM-0120950, by NOAA grant NA17AE1623, NASA grants NAG5-1057 and NAG5-1051, and NSF grant ATM-9527055. Additional support was provided by the National Center for Atmospheric Research which is sponsored by the National Science Foundation.

References

- Akasofu, S. (1981), Energy coupling between the solar wind and the magnetosphere, *Space Sci. Rev.*, *28*, 121–190.
- Boyd, T. J. M., and J. J. Sanderson (1969), *Plasma Dynamics: Application of Mathematics*, 1st ed., Barnes and Noble, New York.
- Boyle, C. P., P. H. Reiff, and M. Hairston (1997), Empirical polar cap potentials, *J. Geophys. Res.*, *102*, 111–125.
- Gonzalez, W. (1990), A unified view of solar wind-magnetosphere coupling functions, *Planet. Space Sci.*, *38*, 627–632.
- Goodrich, C. C., J. G. Lyon, M. Wiltberger, R. E. Lopez, K. Papadopoulos, and J. G. Lyon (1998), An overview of the impact of the January 10–11, 1997 magnetic cloud on the magnetosphere via global MHD simulation, *Geophys. Res. Lett.*, *25*, 2537–2540.
- Kallio, E. J., and H. E. J. Koskinen (2000), A semiempirical magnetosheath model to analyze the solar wind-magnetosphere interaction, *J. Geophys. Res.*, *105*, 27,469–27,479.
- Koskinen, H. E. J., and E. I. Tanskanen (2002), Magnetospheric energy budget and the epsilon parameter, *J. Geophys. Res.*, *107*(A11), 1415, doi:10.1029/2002JA009283.
- Lopez, R. E., J. G. Lyon, M. Wiltberger, and C. C. Goodrich (2001), Comparison of global mhd simulation results with actual storm and sub-storm events, *Adv. Space Res.*, *28*, 1701–1706.
- Palmroth, M., P. Janhunen, T. I. Pulkkinen, and H. E. J. Koskinen (2004), Ionospheric energy input as a function of solar wind parameters: Global mhd simulation results, *Ann. Geophys.*, *22*, 549–566.
- Shue, J.-H., and Y. Kamide (2001), Effects of solar wind density on auroral electrojets, *Geophys. Res. Lett.*, *28*, 2181–2184.
- Siscoe, G. L., G. M. Erickson, B. U. Ö. Sonnerup et al. (2002), Hill model of transpolar potential saturation: Comparisons with MHD simulations, *J. Geophys. Res.*, *107*(A6), 1075, doi:10.1029/2001JA000109.
- Slinker, S. P., J. A. Fedder, B. A. Emery et al. (1999), Comparison of global MHD simulations with AMIE simulations for the events of May 19–20, 1996, *J. Geophys. Res.*, *104*, 28,379–28,396.
- Weimer, D. R. (2001), An improved model of ionospheric electric potentials including substorm perturbations and application to the Geospace Environment Modeling November 24, 1966, event, *J. Geophys. Res.*, *106*, 407–416.
- Wiltberger, M., T. I. Pulkkinen, J. G. Lyon, and C. C. Goodrich (2000), MHD simulation of the magnetotail during the December 10, 1996, sub-storm, *J. Geophys. Res.*, *105*, 27,649–27,663.

S. Hernandez and R. E. Lopez, Department of Physics, University of Texas, El Paso, El Paso, TX 79968, USA. (shernandez@utep.edu; relopez@utep.edu)

J. G. Lyon, Department of Physics and Astronomy, Dartmouth College, 6127 Wilder Laboratory, Hanover, NH 03755, USA. (lyon@tinman.dartmouth.edu)

M. Wiltberger, High Altitude Observatory, National Center for Atmospheric Research, 3450 Mitchel Lane, Boulder, CO 80301, USA. (wiltbemj@ucar.edu)